Stiffness and stress efficiency of periodic reinforcing pads for FPSO's hull

Arthur Lebée, Gilles Forêt

Efficacité en raideur et contraintes de renforts périodiques pour FPSO

Stiffness and stress efficiency of periodic reinforcing pads for FPSO's hull

A. Lebée[1] et G. Foret[1]

1 : Université Paris-Est, Laboratoire Navier (ENPC/IFSTTAR/CNRS).
École des Ponts Paris Tech,
6 et 8 avenue Blaise Pascal.
77455 Marne-la-Vallée cedex2
e-mail : gilles.foret@enpc.fr, arthur.lebee@enpc.fr

Résumé

Les coques de FPSO (Floating Production Storage and Offloading units) subissent une corrosion accélérée à tel point qu'il est nécessaire de les renforcer à l'aide the plaques composites. Lorsqu'il faut couvrir de grandes surfaces ces renforts suivent un motif périodique et ne sont pas connectés entre eux. Ainsi dans ce travail, nous appliquons les concepts de l'homogénéisation périodique à une modélisation éléments finis de la coque et du renfort pour estimer l'efficacité mécanique du dispositif. On montre que pour la plupart des configurations envisagées, les renforts ne sont pas suffisants pour baisser le niveau de contraintes dans la coque. Il est donc préconisé de les connecter entre-eux.

Abstract

The hull of FPSO units (Floating Production Storage and Offloading units) suffers from accelerated corrosion. It becomes now mandatory to restore the original thickness of the hull by means of reinforcing pads. For large areas, the pads follow a periodic pattern and are not connected together. Hence, in this work, we apply plate homogenization techniques coupled with finite elements simulations for assessing the behavior of the pads. It is found that, for most geometric configurations studied here, the pads do not provide sufficient strength reinforcement and requires their mechanical connection.

Mots Clés : Renforts Composites, Homogénéisation des structures
Keywords : Composite reinforcement, Homogenization of structures

1. Introduction

1.1. The Coldpad reinforcement technique

FPSO units store crude oil extracted from subsea wells. They must stay close to the offshore platform between two offloadings to crude oil tankers. Otherwise the production stops and generates large financial losses. It turns out that an accelerated corrosion is observed in many of these vessels : from an original averaged thickness of 17mm for the primary hull, it can drop to 15mm. It becomes then mandatory to restore the original thickness by means of reinforcement devices.
Most reinforcement techniques rely on additional steel sheets which are welded directly on the hull. However, this requires to fully empty the FPSO and ensure that no flammable gas is remaining. Hence, new reinforcement techniques are currently under consideration. One of them is offered by the company "Coldpad®" and is under investigation here. It is based on the use of composites and polymers directly bonded to the hull to be reinforced.

Configuration of a single pad

For a rather localized damage, a single reinforcement pad is bonded to one side of the hull (Figure 1). The in-plane geometry of a single pad is part of other design studies. However, the standard cross section of the reinforcement is as follows. Starting from the hull, there is a rather thick layer of epoxy adhesive in order to accommodate the surface irregularities. Then, there is a thick layer of fiber reinforced composite to which is bonded a thin protection plate. Because epoxy resins are very

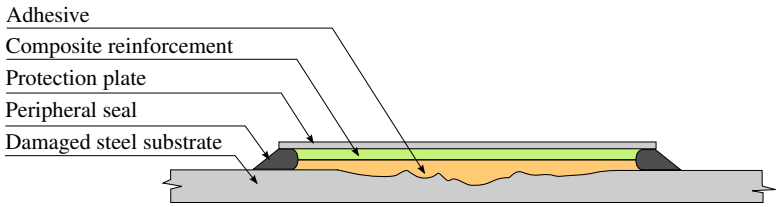

Fig. 1.: Typical cross section of a single pad

sensitive to seawater (swelling), an elastomeric seal goes all around the pad and separates polymer materials from chemical ingression. In addition, the pads will protect the hull from further corrosion. The set-up of the reinforcement is as follows. The pads are prefabricated (composite, protection and seal) and the hull surface is prepared. Then the pads are bonded on-site using infusion techniques. Composites are used in order to reduce the weight of the pads which are carried to the FPSO's damaged area.

Configuration with large damaged areas

There are also large damaged areas. Typical cases are in the water ballast tanks or at the FPSO deck (Figure 3). In this case, it is not possible to have a single pad and a periodic tiling of pads is under consideration (Figure 6). In the present study, the pads are not connected together. Connecting the pads would increase labor. A design without connection would be preferred.

Simple description of the reinforcing effect

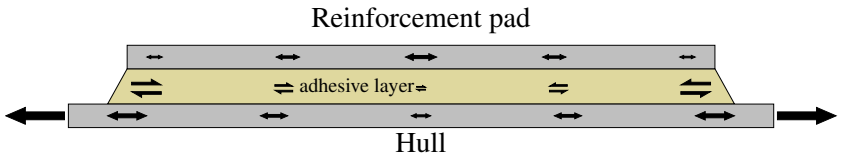

Fig. 2.: Schematic view of the reinforcing effect of the pads.

Without reinforcement, the hull is mostly loaded in its plane (membrane stress). Hence, its design consists mostly in satisfying plastic yielding criterion and out-of plane buckling load.
When adding the reinforcing pads, the adhesive layer sustains mostly transverse shear close to the free edges and transfers longitudinal strains to the composite reinforcement and protection plate (shear lag effect : Figure 2). Thus we expect a decrease of the strain inside the damaged hull and an increase of the bending stiffness of the reinforced hull. Let us point out right away that the reinforcement is added on only one face of the hull. The neutral axis of the hull is shifted in the reinforced area and the real effect of the pad is likely to be more complex than this very simple description.

The approach chosen in this study

There are many questions which needs to be answered regarding this new technology. The design of single pads is already part of other studies. They focus on the optimization of the edges geometry in order to limit stress concentrations. A large campaign of experiments was also performed in order to assess the strength of the pads.
The present study gives a first approach for assessing the behavior of a periodic assembly of pads which covers a large damaged area. Hence, we want to focus on the capability of the pads to actually reinforce the hull in terms of equivalent stiffness and stress inside the hull in the linear regime. Especially, we want to identify potential geometries which work without connecting the pads together. Thus, non-linear effects (like buckling), stress concentrations and creep will be intentionally kept aside for future studies.

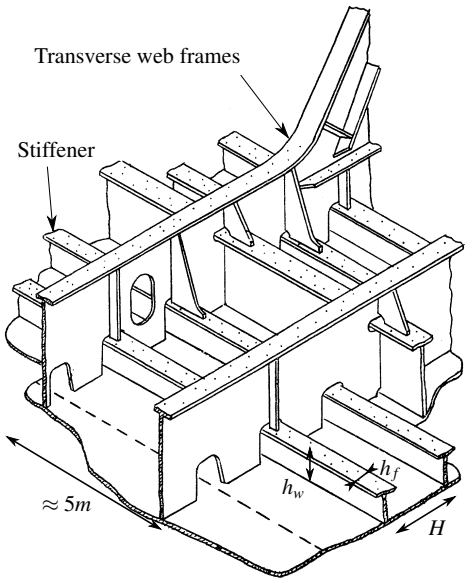

Fig. 3.: Structural detail of the FPSO unit bottom

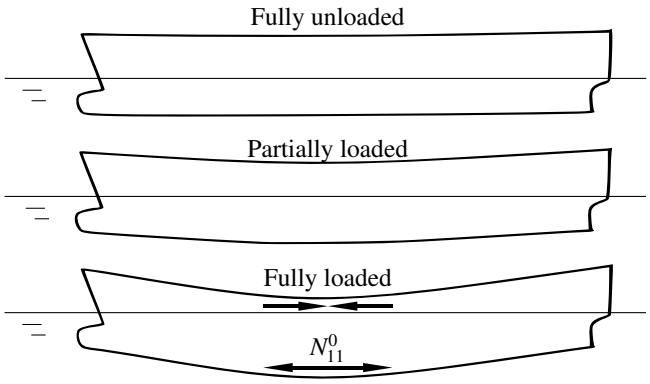

Fig. 4.: Global load of the FPSO

2. Assessment of the reinforcement pads through periodic plate homogenization

2.1. Configuration of the hull to be reinforced

The structural organization of a FPSO is globally as follows. The primary structure is constituted of a succession of transverse web frames from the prow to the poop (Figure 3). They are positioned every five meters in the longitudinal direction. The hull is also reinforced in the longitudinal direction with “T" stiffeners which are about 450 mm height spaced about 1 m in the cross direction.
In this study we consider the case where the damaged area is at the deck of the FPSO. Hence the pads are bonded directly on the hull and tiled according to the stiffeners. For handling reasons, the maximum size of a pad is about 1 m $\times$ 2 m. Between two web frames there will be about 3 to 5 pads. It is not possible to model several pads including the web frames with refined enough FE simulation. Thus, in the following, we assume that a representative periodic pattern includes only the hull, the pads and the stiffeners but not the web frames.

2.2. Periodic plate homogenization in few words

Thanks to this assumption, the assembly of pads is periodic. Thus, homogenization appears as suitable tool for studying the mechanical behavior of the reinforced hull. Homogenization consists in isolating a unit-cell which generates the whole pattern and performing all relevant computations on this unit-cell. The main advantage of this method is that it is not necessary to simulate the whole reinforced area of the hull which reduces significantly the computational burden. In addition, all load cases are treated in the same procedure. It is then possible to try a large number of geometries for the pads.
In the present case, we will homogenize the periodic assembly of hull+stiffeners and reinforcement pads as a simple equivalent plate. At the macroscopic level, a Kirchhoff-Love plate model will be derived. Let us recall that the membrane stress $N_{\alpha\beta}$ and the bending moment $M_{\alpha\beta}$ are the usual generalized stresses for Kirchhoff-Love plates. They work respectively with the associated strain variables : $\underset{\sim}{E}$, the membrane strain and $\underset{\sim}{K}$ the curvature. The homogenization procedure consists in finding the equivalent plate stiffness $\underset{\approx}{A}, \underset{\approx}{B}, \underset{\approx}{D}$, which links the strains $\underset{\sim}{E}$ and $\underset{\sim}{K}$ to the stresses $\underset{\sim}{N}$ and $\underset{\sim}{M}$.
In addition to that, at the microscopic scale, it is possible to relocalize the stress generated by $(\underset{\sim}{E}, \underset{\sim}{K})$ (or $(\underset{\sim}{N}, \underset{\sim}{M})$) inside the unit-cell. All these aspects are extensively detailed in [**? ? ?**]. The key point is to find the solution of auxiliary problems which apply the macroscopic plate loadings ”on average“ on the unit-cell. Finally, those auxiliary problems will be applied to the non-reinforced hull and to the

reinforced hull and the corresponding local fields and equivalent stiffnesses will be compared.

2.3. Stress and stiffness reinforcement rates

In order to estimate the efficiency of the pads we define stress and stiffness rates. Because the homogenization procedure will return six localization fields corresponding to $(\underset{\sim}{E},\underset{\sim}{K})$ or $(\underset{\sim}{N},\underset{\sim}{M})$, we need to specify how the hull is actually loaded.

Choice of the macroscopic load

The loading which mostly sets the design of the FPSO is the weight of the hydrocarbon payload. Whether the vessel is empty of full, this load generates global bending in the longitudinal direction. This means that the bottom of the FPSO is mostly under membrane traction in the longitudinal direction and that this membrane traction is force driven (Figure 4). Hence, let us define N_{11}^0 the macroscopic membrane traction inside the original assembly of hull and stiffeners (without reinforcement). Now that one of the six plate elementary loadings is set, there remains to fix the other five loadings. The answer to this question is actually not straightforward. Assuming there are no web frames, the stiffened hull is free to contract in the cross in-plane direction (in-plane Poisson's effect). The same remark holds for the three curvatures (M_{11},M_{22},M_{12}) and the in-plane shear (N_{12}). Hence without web frames, it seems consistent to let free the other plate loadings :

$$N_{11}=N_{11}^0,\quad N_{22}=0,\quad N_{12}=0,\quad M_{11}=0,\quad M_{22}=0\quad\text{and}\quad M_{12}=0 \qquad \text{(Eq. 1)}$$

We call this macroscopic load configuration "uni-axial traction" (or "load case N").
On the contrary, the web frames restrain to some extent the plate kinematics (except the longitudinal strain E_{11}). Hence we suggest a "dual" macroscopic load configuration defined as "pure axial-strain" (or "load case E") :

$$N_{11}=N_{11}^0,\quad E_{22}=0,\quad E_{12}=0,\quad K_{11}=0,\quad K_{22}=0\quad\text{and}\quad K_{12}=0 \qquad \text{(Eq. 2)}$$

Because the web frames are very close together (every 5m), it is expected that the actual macroscopic load of the plate is closer to uni-axial strain than to uni-axial traction. However, both cases are studied here to be exhaustive.

Definition of reinforcement rates

In this section we define the reinforcement rates for both macroscopic loads.
We define the stress reinforcement rate as the ratio :

$$\tau_\sigma=\sigma^r/\sigma^0 \qquad \text{(Eq. 3)}$$

where, σ^0 is Von Mises stress in the non-reinforced stiffened hull and σ^r is the maximum Von Mises stress with reinforcement. When this rate is lower than 1, the hull is reinforced.
We define also the stiffness reinforcement rate as :

$$\tau_A=\frac{A^r-A^0}{A^{0,s}} \qquad \text{(Eq. 4)}$$

where A^r is the apparent stiffness of the reinforced and stiffened hull for the given macroscopic load, A^0 is the apparent stiffness of the non-reinforced and stiffened hull. Finally $A^{0,s}$ is the apparent stiffness of the hull *without stiffeners*. We choose this stiffness as reference because the we are concerned with the reinforcement of the hull only. The stiffeners are simulated only because their size is comparable to the size of the pads which forces us to include them in the simulations.

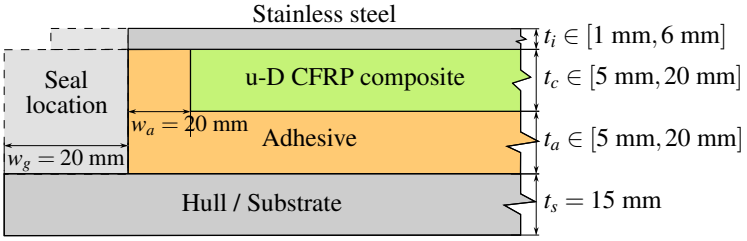

Fig. 5.: Cross section modeled with FE

3. Application to the reinforced hull

3.1. Detailed description of the unit-cell

The hull is made of steel. The Young modulus and the Poisson's ratio are fixed in the whole study to : $E_h = 210\,\text{GPa}$ and $\nu_h = 0.3$. The thickness is also fixed to $t_h = 15\,\text{mm}$. It will be discretized using 3D linear brick elements with reduced integration.
The size of the stiffeners varies in the whole FPSO. It is fixed here to a typical configuration : The web height is $h_w = 450\,\text{mm}$ and its thickness $t_w = 13\,\text{mm}$. The flange total width is $h_f = 75\,\text{mm}$ and its thickness $t_f = 29\,\text{mm}$. The spacing between two stiffeners is set to $H = 925\,\text{mm}$. They are made of the same steel as the hull. In terms of finite elements we choose to model them as shells.
Since the elastomeric seal stiffness is much smaller than the adhesive, it is not modeled at all. In addition, the protection plate overlap over the seal is also not modeled in order to simplify the geometry of the finite element model (Figure 1 and 5).
The adhesive layer is one of the critical part of the design. It is assumed isotropic with a constant Poisson's modulus $\nu_a = 0.4$. Its thickness will vary : $t_a \in [5\,\text{mm}, 20\,\text{mm}]$ as well as its Young modulus : $E_a \in [650\,\text{MPa}, 8000\,\text{MPa}]$. It is discretized with 3D linear elements with reduced integration.
The composite layer will be made of epoxy resin reinforced with glass or carbon fibers. Here we assume uni-directional layup in the longitudinal direction. For the simulations, the composite constitutive law is transversely isotropic. The elastic moduli are derived through the mixture law between moduli of the epoxy matrix ($E_m \in [2\,\text{GPa}, 4\,\text{GPa}]$ and $\nu_m = 0.4$), the fibers moduli and the volume fraction of fibers $\rho_f \in [0.3, 0.5]$ (**?**]). It is discretized with 3D linear elements with reduced integration. The thickness of the composite reinforcement is $t_r \in [5\,\text{mm}, 20\,\text{mm}]$.
The protection plate is assumed to be made of stainless steel. Its thickness is $t_i \in [1\,\text{mm}, 6\,\text{mm}]$. Even if it is well known for having a non-linear constitutive behavior, here we assume that it has a linear and isotropic behavior. The moduli are set to : $E_i = 190\,\text{GPa}$ and $\nu_i = 0.3$.
A typical cross section of the edge of a pad modeled with finite elements is given in Figure 5. For fabrication reasons, there is a gap between the composite and the seal which is filled with adhesive. This gap width is $w_a = 20\,\text{mm}$.
Finally, several in-plane configurations are under consideration. They are introduced in Figure 6. The typical length of a pad is $L = 2000\,\text{mm}$. The width of the seal is $w_g = 20\,\text{mm}$.

3.2. First design – worst case

In this section, we present the results for the case of rectangular pads which were first considered as potential geometries (see Figure 6). It enables us to give the main features of the effect of the pads.

Parameters

We choose the following set of parameters : Adhesive thickness : t_a =5 mm, Stainless steel thickness : t_i =1 mm, Adhesive Young modulus : E_a =8000 Mpa, Composite thickness : t_r =20 mm, Composite longitudinal Young modulus : E_l =117 GPa
The composite reinforcement is quite thick with material characteristics leading to highest moduli.

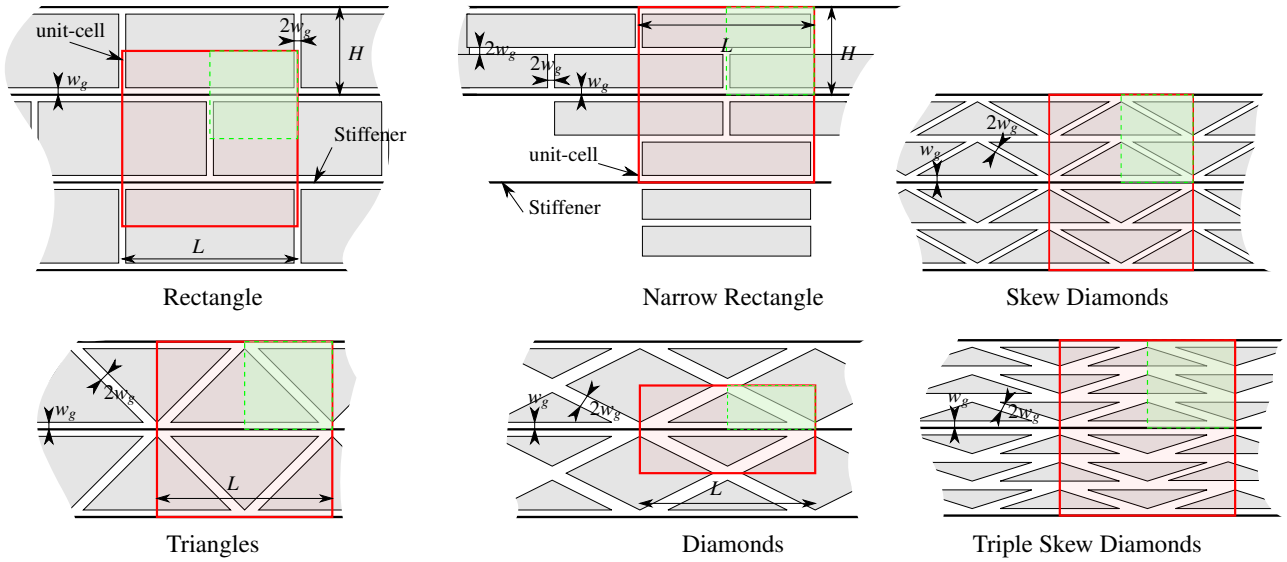

Fig. 6.: The several tilings explored in this study. In red, the unit-cell. In green, the quarter of unit-cell actually simulated.

The adhesive thickness is as thin as possible with a very high modulus. The stainless steel thickness is the thinnest one considered for the design. This first choice of parameters is meant to be as favorable as possible for the efficiency of the pads : thin adhesive layer and thick composite.

Stiffness reinforcement

The following stiffness reinforcement rates are found :
– uni-axial strain : τ_A^E=0.467
– uni-axial traction : τ_A^N=0.457
Hence the average stiffness of the hull is increased around 45% compared to the damaged situation. With this configuration the pad achieves the reinforcement in terms of stiffness.

Stress reinforcement

On Figure 7 is displayed the stress rate field for an assembly of four unit-cells in the uni-axial strain loading case. In most areas, the rate is below 1 which confirms the reinforcing effect of the pads. However, the stress rate jumps just between the pads to rather high values which are :
– uni-axial strain : $\tau_\sigma^E = 2.59$
– uni-axial traction : $\tau_\sigma^N = 2.27$
This is more clearly observed on the right of Figure 7 where only the hull is displayed. A hinge appears along the line which separates two pads. This hinge is generated by two phenomenon. The first one comes from the fact that actually the hull is not reinforced in this region. Then one expect the stress being higher than in the reinforced area. However, one would expect the stress having values close to 1 (the rate without reinforcement). In the present case, the stress rate jumps to values twice larger. When looking more closely at the deformed shape, it appears that the hull is locally bent which generates large local stress. Because the pads are bonded only on one side of the hull, the neutral axis is shifted between reinforced and non-reinforced areas. This eccentricity couples membrane loading and bending. Since the reinforced area is much thicker than the non-reinforced hinge, all the curvature is concentrated in the non-reinforced hinge.
This folding phenomenon critically affects the efficiency of the pads and we seek better geometries in the following. However, let us point out also that in the reinforced area, the stress rate is globally below 84% which illustrates the reinforcing potentialities of the device.

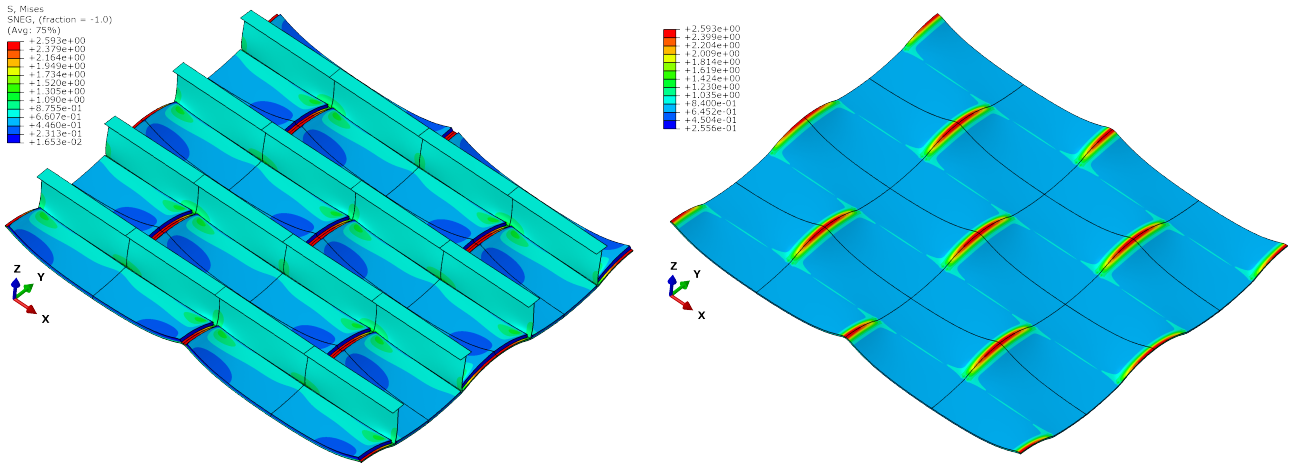

Fig. 7.: Global view of the reinforced hull with rectangular pads. The hull is under uni-axial strain in Direction x and the contour plot is the stress rate. 4 unit-cells are displayed.

3.3. Comparison of in-plane geometries

As already observed, the rectangular shape of the pads leads to local bending between the pads. In this section we explore the influence the the in-plane geometry of the pads in order to identify possibly interesting shapes. We consider the shapes given in Figure 6. Basically we tried to limit the number edges in the cross direction and circumvent the possibilities of folding by not aligning edges. In addition, these geometries must be producible.
In order to compare quantitatively the geometries, we perform a numerical campaign following a factorial experiment. Only parameters related to the thicknesses of the layers and the constitutive behavior are investigated. The values are chosen as the extreme values which can be reached for the design of the pads and where given in Section 3.1.

Stiffness reinforcement

The stiffness reinforcement rate for the uni-axial strain load case is plotted in Figure 8 for each simulation and each geometry. For clarity, the simulations were sorted with respect to the rate of the Rectangle geometry.
The stiffness rate covers a rather broad range from 5% to 50%. In the present study the target is about 10%. The reinforcement rate does not depend strongly on the geometry (all the geometries follow the same trend. Finally, it comes out that the Rectangle geometry is the most efficient in terms of stiffness whereas the Diamond family shows lower rates, especially the Triple Skew Diamond Geometry. A simple explanation for this is that the latter is the geometry which presents the longest perimeter. Hence its reinforcing surface is smaller and the length of free edges for the pads is larger. However, this does not seem to dramatically decrease the stiffness reinforcement rate.

Stress reinforcement rate

The stress rate of all geometries is given for each simulation on Figure 9. Thick lines show the uni-axial strain load case whereas the thin lines give the corresponding rate for the uni-axial traction to be exhaustive. Again the simulations are sorted with respect to the *stiffness* reinforcement rate of the Rectangle geometry. This means that most compliant configurations are located on the left of the figure whereas stiffest configurations are located on the right. The most remarkable observation is that the geometry dramatically affects the stress rate, especially for large stiffness reinforcement. The second observation is that most of the geometries *increase* the stress inside the hull.
More precisely, it appears that the different geometries have different global trends (increasing or not

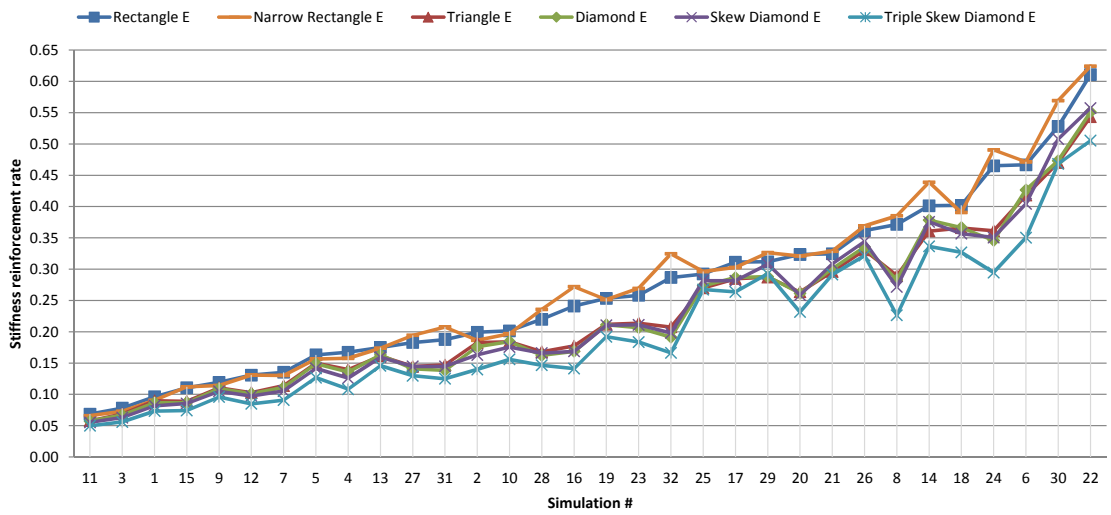

Fig. 8.: Stiffness rate inside the hull for each simulation and each geometry. The simulations are sorted from left to right with respect to the stiffness rate of the Rectangle configuration.

from left to right) but follow similar local patterns depending on the change of parameters between each simulation. We conclude that the local patterns are the consequence of fine tuning of parameters which will be investigated later on, whereas the global trend shows the influence of the in-plane geometry and is discussed here.
Considering the Rectangle geometry, the stress rate increases when the stiffness rate increases (the stress rate is larger for simulations on the right of the figure). This means that increasing the stiffness and decreasing the stress are antagonistic demands. This is because of the hinge phenomenon already described : the more the hull is reinforced, the thicker is the pad, the more local is the hinge, the larger is the bending stress. We conclude that the Rectangle geometry will never lead to a suitable design. The same remark holds for the Triangle and Diamond geometries even if the effect is smaller.
The only geometries for which the stress rate does not clearly increase with the stiffness are the Skew Diamonds and the Triple Skew diamonds. Actually these are also the only one which are close to reinforcing the hull (stress rate below 1).

Conclusion regarding the in-plane geometry

Performing the same simulations for different in-plane geometries points out that they do not affect significantly the stiffness reinforcement rate. This design criteria is affected by other parameters which will be investigated in the following. However, the geometry critically affects the stress rate. The hinge phenomenon is present in almost all situations and leads to an antagonistic demand between increasing the stiffness and decreasing the stress inside the hull. Finally, only the Triple Skew Diamond seems to have potentialities. Consequently, we select this geometry in the following for optimizing the design and investigating the influence of the remaining parameters. Let us already point out that this geometry is much more complex than the one of the rectangle.

3.4. Investigation of the Triple Skew Diamond Geometry

In order to have a comprehensive description of the possibilities of this geometry, we performed the same factorial experiment as in the previous section to which we added two values for the length of the pad : $L = 2000$ mm and $L = 2500$ mm. We investigate longer pads than firstly considered since it will turn out to be a critical parameter.

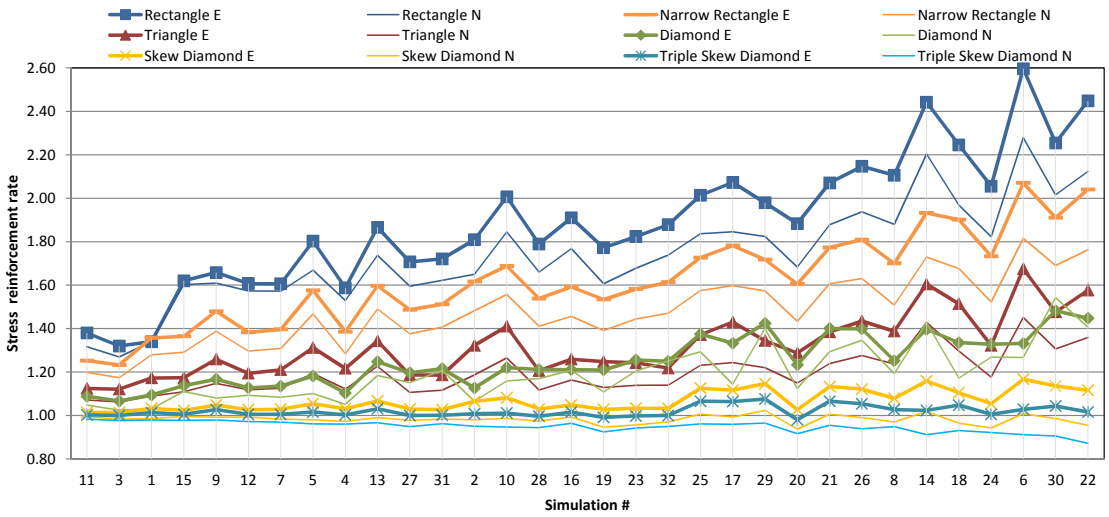

Fig. 9.: Stress rate inside the hull for each simulation and each geometry. The simulations are sorted from left to right with respect to the stiffness rate of the Rectangle configuration (like Figure 8).

Overview of results

On Figure 10 is given the stress reinforcement rate as function of the stiffness reinforcement rate for all simulations and for both load cases. Clearly, the most restrictive load case is the uni-axial strain and the uni-axial traction leads to much lower stress rate. Contrary to the other geometries, here the stress rate *decreases* globally with larger stiffness reinforcement rate which is the expected reinforcement effect. However, the achieved stress reinforcement are rather low : 0.944 for the best case in uni-axial strain.

Parameters influence

A simple procedure was applied to bring out the influence of the parameters. Considering one parameter, for each of its values investigated we compute the average all simulations (the other parameters varying). The average is performed for the two rates. Because we have a factorial experiment, for each value of a single parameter, the average is performed on exactly the same set of remaining parameters. The results are given on Figure 11. The graphs are organized in three rows corresponding to both reinforcement rates. The columns correspond to each investigated parameters.
Globally, there is a clear distinction between the load cases only for the stress reinforcement rates (the gap being 7% on average) whereas results are almost identical with the stiffness rate. This is because the uni-axial strain enforces more kinematic constraints on the unit-cell than the uni-axial traction.
Let us consider the stiffness reinforcement rate. The stainless steel thickness t_i and the composite thickness t_r have a clear positive effect on the stiffness reinforcement. In addition high tensile characteristics for the composite and high adhesive modulus are also favorable to the stiffness rate. These influences are quite expectable. It is noticeable that the length of the pad L and the thickness of the adhesive have less influence on the stiffness rate. This tends to indicate that the shear lag effect (Figure 2) is not so large.
Because the stress reinforcement rate is highly correlated to the stiffness reinforcement rate (cf. Figure 10) the same influences of the parameters would be expected on the stress rate. However, this is not exactly the case. The positive influence of the tensile characteristics of the composite and of the composite thickness on the stress rate is confirmed. Similarly, the adhesive thickness does not seem to critically affect the stress rate. However, the influence of the stainless steel thickness and the adhesive modulus is less clear and the influence of the length of the pad is stronger than for the

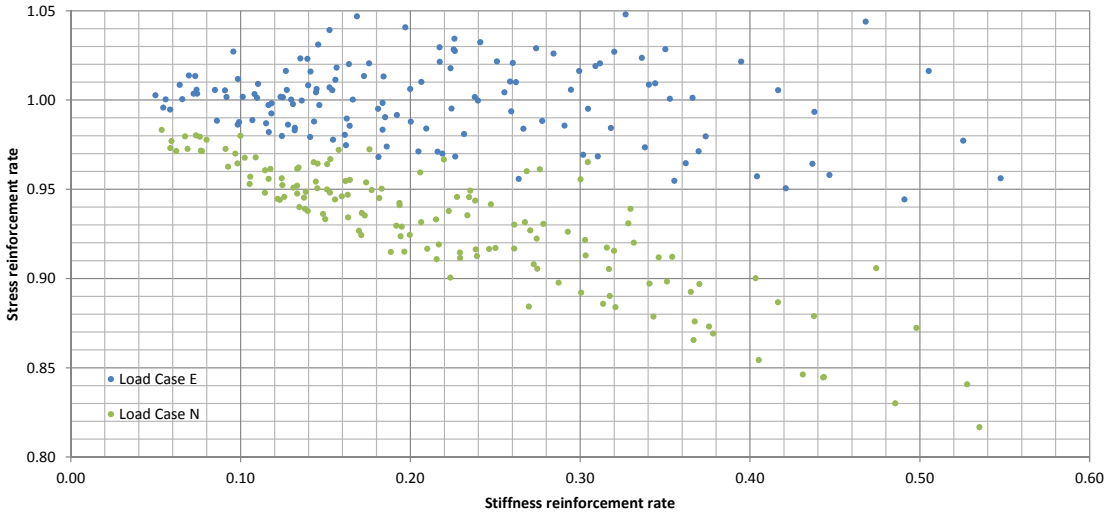

Fig. 10.: Stress reinforcement rate vs. Stiffness reinforcement rate for the Triple Skew Diamond factorial experiment

stiffness rate. The stainless steel thickness has a favorable effect on the stress rate because it increases the stiffness of the hull. However, it has a negative effect because it increases the bending stiffness of the pad. When the pad bending stiffness increases, it localizes the curvature along the hinges coming from the gap between pads. This effect is stronger than with the composite layer. This is because the composite layer is strongly anisotropic : the very compliant transverse shear stiffness of this layer accommodates more easily the hinge. Hence it seems more preferable to increase the thickness of the composite layer than the thickness of the stainless steel. The influence of the adhesive modulus is also ambiguous. High moduli should decrease the stress rate because they increase the stiffness rate. However, the opposite trend is observed for the uni-axial load case. Further analysis of the results shows that the best reinforcing rates are achieved for $E_a = 3000\,\text{MPa}$ which shows that there is probably an optimum value to be found. Finally, when the pads length increases, the hinge are more oriented in the longitudinal directions. This might explain the larger influence of this parameter.

3.5. Design recommendations

In the light of the present study, it possible to express some recommendations for the design of reinforcing pads not connected together.

The first point is that the geometry critically affects the stress reinforcement rate. Because the pads are not connected, there is a shift of neutral axis which generate local hinges between pads. Exploring potential geometries shows that the Triple Skew Diamond one mitigate enough this phenomenon. One cannot exclude other potential geometries which might be more efficient. However, they must be suitable for fabrication.

One question was to check if the rather large thickness of the adhesive layer would generate a large shear lag effect and preclude any reinforcement. This effect is present, however it is not dominating the behavior of the pad (for the length considered here). Thus, having rather thick and compliant adhesive layer does not compromise the strengthening effect of the pad. On the contrary it might be beneficial since it accommodates the hinge phenomenon. Having $t_a = 20$ mm and $E_a = 3000$ MPa seems a good compromise.

Finally, from the parameters influence study it appears that it is preferable to reinforce with composite than with stainless steel because the transverse shear compliance of the composite accommodates better the hinge phenomenon. In addition, the composite should have the highest tensile properties in order to maximize its reinforcing effect.

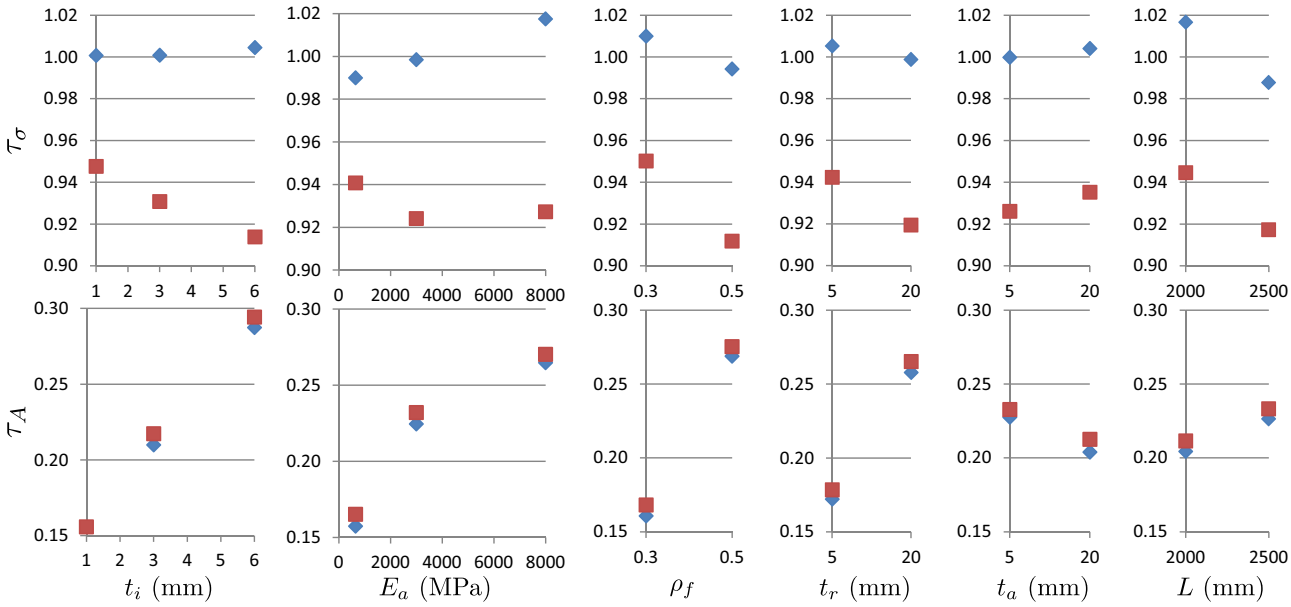

Fig. 11.: Sensitivity analysis for the Triple Skew Diamond factorial experiment. Blue markers are for the uni-axial strain and brown markers for the uni-axial traction load cases.

4. Conclusion

The present work shows the application of homogenization techniques in the linear elastic regime, in order to assess the efficiency of periodically tiled reinforcing pads. The following conclusion are drawn :

– The pads are able to restore the original stiffness of the hull.
– The pads efficiency in terms of stress reduction is very low. This is because the pads shift the neutral axis of the hull and generate local hinges.

Hence, even if it were possible to decrease the stress inside the hull, this would generate a very large increase of the local stiffness (see Figure 10) and would seriously perturb the global behavior of the hull. In addition, we focused on the longitudinal load for the sake of simplicity but there are other load directions which will require investigation and for which the Triple Skew Diamond geometry will not be suitable.

Consequently, it is highly recommended to connect mechanically the pads together in order to achieve a continuous reinforcement.

Références

[] D. Caillerie « Thin elastic and periodic plates », *Mathematical Methods in the Applied Sciences* Vol. 6 n° 1, pp. 159–191, 1984, ISSN 01704214.

[] A. Lebée, K. Sab « Homogenization of thick periodic plates : Application of the Bending-Gradient plate theory to a folded core sandwich panel », *International Journal of Solids and Structures* Vol. 49 n° 19-20, pp. 2778–2792, 2012, ISSN 00207683.

[] A. Lebée, K. Sab « Homogenization of a space frame as a thick plate : Application of the Bending-Gradient theory to a beam lattice », *Computers & Structures* ISSN 00457949.

[] D. Gay, Composite materials : design and applications, ISBN 1587160846, 2003.